JOURNAL OF Materials CHEMISTRY

β″-(ET)$_3$(MnCl$_4$)(1,1,2-C$_2$H$_3$Cl$_3$) (ET = bis(ethylenedithio)tetrathiafulvalene); a pressure-sensitive new molecular conductor with localized spins†

Toshio Naito,*[a] Tamotsu Inabe,[a] Keiji Takeda,[b]‡ Kunio Awaga,[b] Tomoyuki Akutagawa,[c] Tatsuo Hasegawa,[c] Takayoshi Nakamura,[c] Toru Kakiuchi,[d] Hiroshi Sawa,[d] Takashi Yamamoto[e] and Hiroyuki Tajima[e]

[a]*Division of Chemistry, Graduate School of Science, Hokkaido University, Sapporo 060-0810, Japan. E-mail: tnaito@sci.hokudai.ac.jp*
[b]*Department of Basic Science, The University of Tokyo, Japan*
[c]*Research Institute for Electronic Science, Hokkaido University, Japan*
[d]*Department of Physics, Chiba University, Japan*
[e]*Institute for Solid State Physics, The University of Tokyo, Japan*

Received 27th March 2001, Accepted 30th May 2001
First published as an Advance Article on the web 2nd July 2001

An electrolysis of bis(ethylenedithio)tetrathiafulvalene (ET) and a Mn-cluster in a 1,1,2-trichloroethane solution containing 10% (vol/vol) of ethanol yields black lustrous single crystals, β″-(ET)$_3$(MnCl$_4$)(1,1,2-C$_2$H$_3$Cl$_3$) based on the X-ray structural study. The crystal structure can be characterized as alternating two-dimensional donor sheets and insulating sheets made of isolated $[MnCl_4]^{2-}$ ions and the 1,1,2-C$_2$H$_3$Cl$_3$ molecules. Every pair of the neighbouring donor molecules has a large displacement along both short and long molecular axes. A tight-binding band calculation suggests that this arrangement should lead to a weak but isotropic intermolecular interaction in the donor sheets, and this in turn should lead to a marginally metallic or semiconducting electronic structure. Although the polarized reflectance spectra and the temperature-dependent spin susceptibility derived from the EPR spectra on the single crystal indicate metallic nature, the electrical behaviour under atmospheric pressure is semiconductive with room temperature conductivity of 35 S cm^{-1} and apparent activation energy of 0.023 eV. It exhibits a resistive hump with hysteresis at around 60 K, which could be associated with a structural transition demonstrated by a series of low temperature X-ray oscillation photographs. The magnetic susceptibility at 4.5–300 K does not exhibit any anomaly and is well reproduced by the Curie–Weiss model with Curie constant C/emu K mol^{-1} = 3.89 and Weiss temperature θ/K = −0.10. This magnetic behaviour can be quantitatively understood as the sum of Pauli paramagnetism of the π-electrons and the contribution from the local spins on the Mn(II) ions with d^5-configuration (S = 5/2). High pressure easily suppresses the increase in resistivity at low temperature, and the electrical behaviour is particularly sensitive to the first 3–5 kbar.

Introduction

The research of molecular functional crystalline materials with conducting or magnetic properties has now reached the stage where few researchers would find it surprising for a molecular material to exhibit superconducting or ferromagnetic properties at low temperature.[1] The next step could be the search for an advanced material based on characteristics which would not be realized unless the material is a molecular crystal. Examples of such endeavour may include the worldwide attempts to combine some of the properties which would be sometimes incompatible in other materials. In particular the molecular conductors with localized spins have been most intensively studied, and such study has made a steady progress in recent years.[2–8]

Although many researchers have been making every effort towards enhancement of the interaction between local spins and conduction electrons, we have paid much attention to the characteristic weakness of intermolecular interaction in the crystalline materials. Such weak interactions can be comparable to the magnitude of easily available perturbations such as a magnetic field, light, high pressure and stress. Therefore this characteristic enables us to easily, widely modulate and control their physical properties, which might form a striking contrast to other classes of materials. If the conduction electrons weakly interact with the localized spins, subtle energy balance among the lattice, conduction electrons and local spins would make the phase-diagram complex. Such a material might allow a rare combination of electrical and magnetic properties to coexist, or might exhibit a wide variety of electrical and magnetic properties with the variation in temperature, pressure and magnetic field.

In the course of searching for such molecular materials a Mn-cluster has drawn our attention as a good candidate of the counter ion for chalcogen donor-molecule complexes because of the following properties: the Mn-cluster has been reported to exhibit a high-spin state (S = 9–14)[9–12] and unusual magnetic properties[13,14] as a "single molecular magnet". Therefore if it would exhibit the unusual magnetic properties in metallic charge-transfer salts of a chalcogen-donor molecule, the resultant electronic system might behave as described above. However the straightforward electrochemical synthesis starting

†Electronic supplementary information available (ESI) available: the temperature dependence of the intensity ratio between fundamental and superlattice spots; $I(-2,10,9)/I(2,20,6)$ (Fig. S1), intermolecular short distances (Table S1), selected bond lengths and angles (Tables S2 and S3). See http://www.rsc.org/suppdata/jm/b1/b102786g/
‡Present address: Division of Chemistry, Graduate School of Science, Hokkaido University, Sapporo 060-0810, Japan.

DOI: 10.1039/b102786g

from bis(ethylenedithio)tetrathiafulvalene (ET) and the Mn-cluster resulted in decomposition of the cluster and the solvent used, and we obtained the title compound. Fortunately the obtained material has been found to exhibit peculiar physical properties which could be associated with some of the intended properties mentioned above. Herein we describe the unique structural, electrical, optical and magnetic properties.

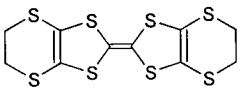

ET ($C_{10}H_8S_8$)

Experimental

Synthesis

The Mn-clusters were synthesized by the reported method.[9–11] Bis(ethylenedithio)tetrathiafulvalene (ET) was purchased from Tokyo Chemical Industry Co., Ltd. and used as received. Single crystals were obtained from a standard electrochemical oxidation of ET (14 mg) in 1,1,2-trichloroethane (TCE) containing 8–10 vol% of C_2H_5OH (50 ml solution in total) with the neutral ($[Mn_{12}O_{12}(C_6H_5COO)_{16}(H_2O)_4]$; 20 mg) and the monoanionic Mn-clusters ($[(C_6H_5)_4P][Mn_{12}O_{12}(C_6H_5COO)_{16}(H_2O)_4]$; 40 mg) under a nitrogen atmosphere. The current was kept constant at 1.3–2.5 μA for 2–3 weeks at room temperature. IR(cm^{-1}): 1420.0, 690.6, 668.7, 488.2, 472.7. Elemental analysis $C_{32}H_{27}S_{24}MnCl_7$ (calc) C 25.90; H 1.83; N 0.00; S 51.85; Cl 16.72, (found) C 26.54; H 2.10; N 0.00; S 51.34; Cl 16.02%.

Physical properties

All the measurements were carried out immediately after the filtration of the single crystals, which were quickly identified to be the desired product of sufficiently good quality by X-ray photographs using a Rigaku Imaging Plate.

X-Ray crystallography§

A selected single crystal was glued on a glass fibre and the reflection data collection was carried out with a Rigaku R-AXIS RAPID Imaging Plate area detector with graphite monochromated Mo-Kα radiation ($\lambda = 0.7107$ Å) at room temperature. The intensities were corrected for Lorentz and polarization effects. Empirical absorption correction was applied. The structure was solved by a direct method,[15] and the hydrogen atoms were placed at the calculated ideal positions. A full-matrix least-squares technique on F with anisotropic thermal parameters for non-hydrogen atoms and isotropic ones for hydrogen atoms was employed for the structure refinement. Hydrogen atoms were included but not refined. Atom scattering factors were taken from the literature.[16] The values for the mass attenuation coefficients are those of Creagh and Hubbell.[17] All calculations and a part of the molecular graphics were performed using the teXsan[18] crystallographic software package from Molecular Structure Corporation and some structural views are produced using Ortep3 for Windows.[19] The final values of refined atomic parameters with esd's, bond lengths and angles together with other details of the experimental conditions are deposited in a CIF file as supporting information. Crystal morphology was identified by a Rigaku AFC-7R 4-circle diffractometer.

A low temperature structural study was carried out using standard home-made X-ray-photograph equipment or at KEK Photon Factory (BL-1B). A needle-shaped specimen of 1–4.5 mm long was mounted on a sapphire rod with apiezon grease N and H (1 : 1 mixture) and was preliminarily checked by 31 X-ray photographs at room temperature immediately before cooling. The cooling–heating rate was 1 K min^{-1} (300–200 K), 0.67 K min^{-1} (200–100 K) and 0.5 K min^{-1} (100–13.6 K). The oscillation angle was 6.5 degree and each exposure time was 300 s. First we took the oscillation photographs at every 5 K from 13.6 K to 50 K (heating 1), then at every 5 K from 50 K to 13.6 K (cooling) and then at every 5–20 K from 13.6 K to room temperature (heating 2). The temperature dependence of the intensity ratio between fundamental and superlattice spots; $I(-2, 10, 9)/I(2,20,6)$ (Fig. S1), intermolecular short distances (Table S1), selected bond lengths and angles (Tables S2 and S3) are deposited as ESI.†

Electrical properties

The electrical resistivity was measured using a standard direct-current 4-probe method with gold wires and gold paints, and a Be/Cu clump-type cell on high-pressure measurements. The pressure medium used was Daphne oil 7373 (Idemitsu Co., Ltd.). The applied pressure values were measured at room temperature and not corrected for solidification and thermal contraction of the pressure medium at low temperature. The current was applied along the [10$\bar{1}$] direction on the most-developed facet (*ac*-plane) of a single crystal. The measurements were carried out using a home-made personal computer-controlled cryostat system. The system is made of (1) an insertion with a high-vaccum jacket and a pumping/He inlet valve, (2) Hewlett Packard universal source 3245A, (3) Hewlett Packard 34401A multimeter, (4) Hewlett Packard nanovolt/microohm meter 34420A, (5) Advantest Programmable DC voltage/current generator TR6142, (6) Keithley 2000 multimeter and (7) LakeShore Autotuning 330 temperature controller with Silicone Diode DT-470-SD. Linearity between applied current and observed voltage drop in a sample was checked at every start of the measurements.

Magnetic susceptibility

A few mg of single crystals (*ca.* 20–30 in number; every single crystal was briefly checked by X-ray oscillation photographs in advance and identified as the desired crystal of high quality) were selected and set in a SQUID susceptometer (MPMS-5S of Quantum Design) with a field strength of 0.8–1.5 T. The linearity of magnetization up to 5.0 T was checked at 5 K by measuring the magnetization curve. The examined temperature range was 4.5–300 K and the diamagnetic correction was carried out using the observed value for an ET molecule and by the Pascal law for the other species.

EPR spectra

The electron paramagnetic resonance spectra of the X-band (9.3 GHz) were measured on the single crystal in the temperature range 3.6–300 K using an EMX EPR spectrometer (Bruker) equipped with a continuous flow cryostat ESR 900 (Oxford). The temperature was controlled so as not to allow the temperature variation to exceed ±0.5 K or ±1% of the set value during the field sweep. An elongated plate-shaped crystal was mounted on a Teflon rod, settled with a minimum amount of grease and sealed in a 5 mm diameter quartz tube in a helium atmosphere of *ca.* 20 Torr. The Teflon rod was also settled at the bottom of the quartz tube with a minimum amount of grease. The quartz tube was equipped with a circular protractor and the anisotropy of the spectra were examined within a ±1° accuracy by rotating the quartz tube about the long axis of the specimen, which nearly coincided with the [10$\bar{1}$] direction. The measurement was carried out on several samples with different

§CCDC reference number(s) 163869. See http://www.rsc.org/suppdata/jm/b1/b102786g/ for crystallographic files in .cif or other electronic format.

conditions and the signal was checked to ensure saturation had not occurred at 3.6, 70 and 297 K at every measurement.

Reflectance spectra

A rectangular platelet single crystal with sufficient quality and most developed crystal facet of the *ac*-plane was selected based on X-ray oscillation photographs. The measurements were carried out using a Fourier transform infrared micro sampling spectrometer JASCO FT-IR-8900μ equipped with microscope MICRO 20 at room temperature. Polarization directions were determined within $\pm 5^{\circ}$ accuracy as the two directions that gave lowest and highest reflection at lower wavenumber region from actual measurements. The two directions of the polarization were perpendicular to each other and thus called 0 and 90 degrees below unless there can be any possibility of misunderstanding. The 0°-direction coincided with the long edge of the rectangle and X-ray photographs suggested that this was nearly parallel to the [10$\bar{1}$] direction. The best specimen, however, did not have smooth mirror surfaces. Therefore note that the result should be regarded as a preliminary one and detailed quantitative discussion should wait for the measurement on a single crystal with a mirror surface.

Results and discussion

Synthesis

Little change in the solution was observed during the first week of the electrolysis, and this indicates that firstly the decomposition of the cluster and solvent molecules occurs then the crystallization should follow. However, use of $[(C_2H_5)_4N]_2$-$[MnCl_4]$ instead of the Mn-cluster salt did not yield the title compound under the corresponding electrolytic conditions. Single crystals of an ethanol-coordinated Mn-cluster were sometimes obtained along with the desired product, and this suggests that ethanol might induce the decomposition of the original Mn-cluster.

Molecular, crystal and electronic structures

The crystallographic data and experimental conditions are tabulated in Table 1. The crystal structure is depicted in Fig. 1. It consists of alternating conduction and insulating sheets parallel to the *ac*-plane. The former is made of three-fold stacked ET molecules along [10$\bar{1}$] but the three-fold periodicity is obscure judging from the interplanar distances and relative molecular displacements (Fig. 2(a)). There are intermolecular short distances comparable to the sum of the van der Waals radii between the neighbouring ET molecules in different columns (between S–S, S–C, C–C and S–H atoms: see Table S2). The rather two-dimensional (2D) molecular arrangement and the characteristic large displacement between every two overlapping molecules (Fig. 2(b)) are designated as β''_{33}, which is the first example among many known β''-type chalcogen-donor arrangements.[20] The β''-type donor-molecular arrangement is now attracting increasing attention because a series of recently discovered organic superconductors have this donor arrangement in common[3,4,21,22] which is reminiscent of the previous successive appearance of the κ-type organic superconductors.[1]

Table 1 Crystal structure determination, conditions and unit cell parameters

Formula	$C_{32}H_{27}S_{24}Cl_7Mn$
FW	1484.11
T/K	296.2
Crystal system	Monoclinic
Lattice type	Primitive
Space group	$P2_1/m$ (No. 11)
a/Å	9.9182(5)
b/Å	29.591(2)
c/Å	10.1562(5)
β/deg	109.443(2)
V/Å^3	2810.8(2)
Z	2
Cryst color/habit	Black plate
Dimensions/mm^3	$0.70 \times 0.10 \times 0.02$
D_{calcd}/gcm^{-3}	1.753
μ (Mo-Kα)/cm^{-1}	14.88
F(000)	1494.00
No. of reflections	
Measured (total)	5946
Observed($>3\sigma(I)$)	2322
R_{int}	0.066
Variables	298
Corrections	Lorentz-polarization
GOF on *F*	4.39
R, R_w	0.078; 0.089 (both for all data)

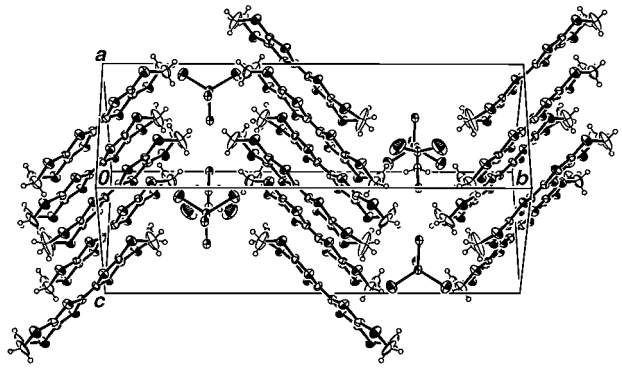

Fig. 1 The crystal structure of $(ET)_3(MnCl_4)(TCE)$.

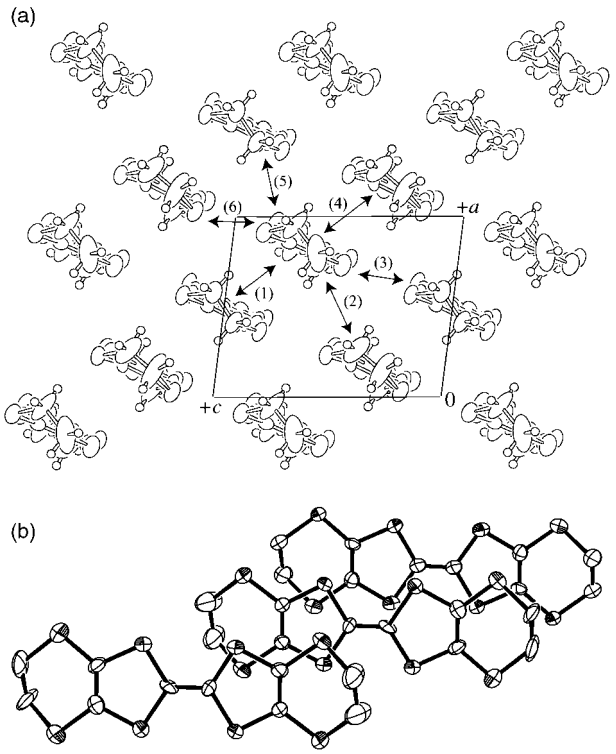

Fig. 2 (a) Donor molecular arrangement and calculated overlap integrals (*S*) of the conduction sheet in $(ET)_3(MnCl_4)(TCE)$: $S \times 10^{-3} = (1)$ 10.6, (2) 19.0, (3) 9.5, (4) −2.7, (5) 11.4, (6) −8.1. Intermolecular S–S short contacts (< 3.7 Å) are found between the two donor molecules connected by the arrows (2), (3), (5) and (6). (b) Donor molecular overlapping modes: the hydrogen atoms are omitted for clarity.

All the donor-molecule long axes are parallel in a sheet, while nearly perpendicular to each other in the two neighbouring sheets. The insulating layers contain the solvent (TCE) molecules and almost regular tetrahedral $MnCl_4$ anions. They both are on the mirror planes without any disorder or non-integral stoichiometry. The $MnCl_4$ anion is considered to be $[MnCl_4]^{2-}$ based on its geometry, *i.e.* bond lengths and angles compared with previous work.[23,24] This interpretation is consistent with the charge estimation of the donor molecules and also consistent with the magnetic property (see below). There are some interatomic contacts no longer than van der Waals distances between the S atoms in ET and the Cl atoms in $MnCl_4$ or TCE species. In addition there are also intermolecular short contacts involving hydrogen atoms, *i.e.* between the H atoms in ET and the Cl atoms in $MnCl_4$ or TCE species.

As for the molecular structures, two kinds of ET molecules are crystallographically independent and one is located on an inversion centre. But a close examination showed no significant differences in the two independent molecular structures. This suggests that the charge should distribute almost equally over the ET molecules, *i.e.* $ET^{0.66+}$; this interpretation agrees with previously reported relations between bond lengths and charges on the ET molecule.[25,26] The samples were somewhat unstable in air for an unknown reason. The storage of the single crystals in a tightly sealed glass micro-tube at $-30\,^{\circ}C$ kept them in a good condition for several weeks. The crystals, however, rapidly and extensively deteriorated on storage in the solvent even at $-30\,^{\circ}C$.

A tight-binding calculation of overlap integrals between the HOMO's (highest occupied molecular orbitals) of the donor molecules indicates that they interact with each other more closely through the side-by-side directions rather than in the stacking direction (Fig. 2(a)). In fact the calculated overlap integrals suggest that intermolecular interaction in the conduction sheet should be two-dimensional. If we suppose that every ET cation radical should have the same charge (+0.66), the tight-binding band calculation suggested that the Fermi level would be a tangent to the energy dispersion curve of the upper band, and the energy gap is about 0.02 eV. Noting that the actual charge on average should be plus two-thirds, *i.e.* marginally larger than +0.66, the calculation implies that this material might be marginally metallic or semiconducting with a fairly small energy gap. This argument agrees well with the observed high conductivity and the small temperature dependence of it. In addition the band gap, if any, is so small that the slightest perturbation such as variation in temperature and pressure could result in a drastic change in the conducting behaviour (*vide infra*).

A series of X-ray oscillation photographs taken at low temperature proved that a first-order transition occurred around 40–60 K accompanied by the *c*-axis doubling and hysteresis and with some sample dependence. The X-ray photograph taken at 13.6 K clearly shows extra spots due to the *c*-axis doubling as shown in Fig. 3. The extra spots were observed at all temperatures below *ca.* 50 K and re-entrant behaviour was not observed in the structural transition. No anomalies in the temperature dependence of the other lattice parameters were observed; they only exhibited continuous thermal contractions down to 14 K. Interestingly the doubling of the *c*-axis does not have anything to do with opening or widening an energy gap at the Fermi level of this compound; this structural transition must be explained other than in terms for a simple metal–insulator transition. The transition temperature (T_c) dependence on cooling/heating rate was not examined. A connection between the physical properties described below and structural transition will be clarified after the structure determination at low temperature, which is now under way.

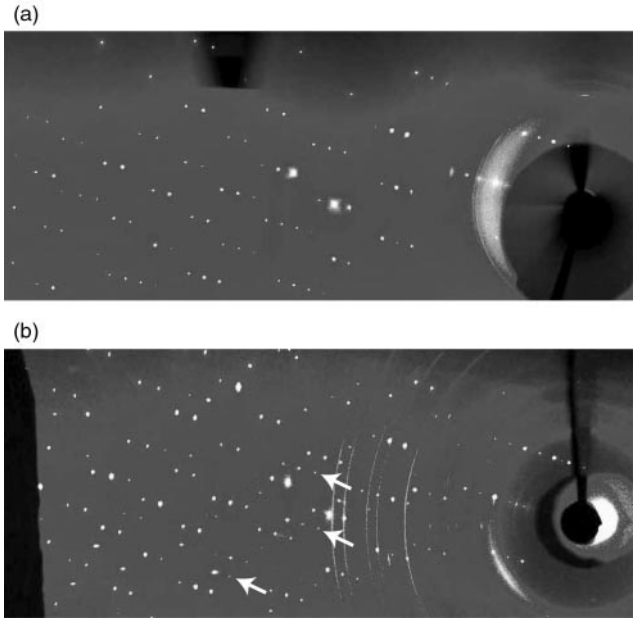

Fig. 3 The X-ray photographs taken at 300 K (a) and 13.6 K (b): the latter shows the extra spots due to the *c*-axis doubling.

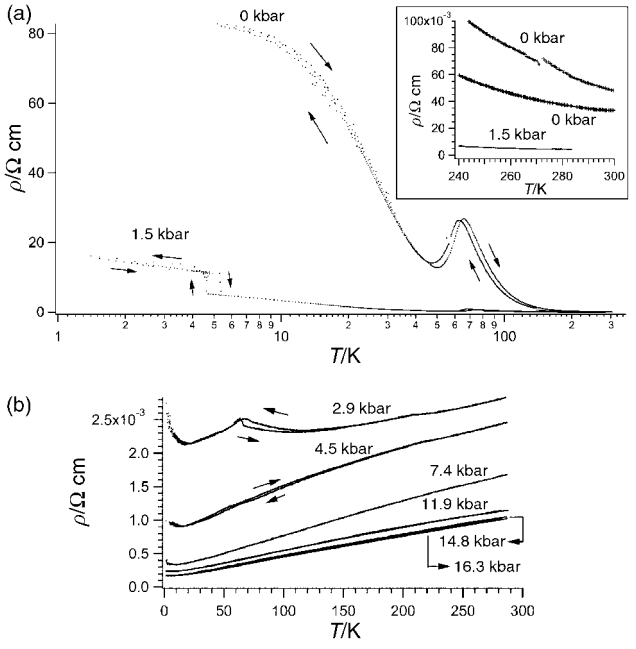

Fig. 4 The electrical behaviour of $(ET)_3(MnCl_4)(TCE)$ under (a) ambient and 1.5 kbar and (b) higher pressures (the indicated pressure values were measured at room temperature and were not corrected for solidification and thermal contraction of the pressure medium at low temperature).

Electrical properties

The electrical behaviour of $(ET)_3(MnCl_4)(TCE)$ is shown in Fig. 4. It exhibited semiconducting behaviour as a whole with a room temperature conductivity of 35 S cm^{-1}. The behaviour at higher temperature ($\gtrsim$80 K) can be approximately described by activation law, and the apparent activation energy from the temperature range 83.33–285.7 K is 0.023 eV. Under ambient pressure the resistivity was almost temperature-independent at high temperature, while it monotonically and gradually increased at temperatures lower than *ca.* 50 K. Since the resistivity at 5 K is still very low and the slope of the increase in resistivity decreases near the lowest temperature of the measurement as if the resistivity has started to saturate, the

electrical behaviour could hardly be regarded as that of semiconductors or insulators. In addition, the resistivity had a clear maximum around 60 K accompanied by a hysteresis.

A transition-like increase in resistivity appeared at 5 K under 1.5 kbar, then it was suppressed rapidly on increasing pressure: note the drastic change in temperature-dependence of the resistivity within the first 3 kbar. The origin of the transition might be due to the structural transition mentioned above but this is yet to be clarified. However, since the structural transition in this case does not result in opening an energy gap at the Fermi level as mentioned above, the electrical conduction mechanism might remain unchanged below and above the T_c at ambient pressure. No qualitative change in conduction electrons' character would leave the magnetic susceptibility without anomalies around 50 K (discussed below). While the resistive anomaly at 60–70 K was gradually suppressed on increasing pressure, another small anomaly manifested itself at 210–220 K. In order to clarify what occurs under high pressure the measurement of the magnetic susceptibility under high pressure will be required.

Magnetic properties

The temperature dependence of the magnetic susceptibility χ_p after the correction for diamagnetic contribution exhibited no anomalies around 50 K (Fig. 5) and was well reproduced by the Curie–Weiss model [see eqn. (1)] through 4.5–300 K using the following parameters; Curie constant C/emu K mol^{-1} = 3.89, Weiss temperature θ/K = −0.10.

$$\chi_p = \frac{C}{T-\theta} \quad (1)$$

This means that the magnetic interaction is negligibly small in this compound. As the $MnCl_4$ anions are well separated from each other in the crystal, possible magnetic interactions involving localized spins depend on the strength of the interaction between the $[MnCl_4]$ anions and the conduction electrons in the ET sheets. Accordingly if this interaction is small, the spins on the $MnCl_4$ anions would be expected to exhibit Curie-like behaviour. In addition, such a case often gives a Curie constant corresponding to the sum of the contribution from the total spins. The value C corresponds to 89% of Mn^{2+} spins (d^5, $S = 5/2$) if the g-value is assumed to be 2.000. This magnetic behaviour coincides with that of $[\{(C_6H_5)_3P\}_2N][MnCl_4]$ (C/emu K mol^{-1} = 3.89, θ/K = −0.25), which also contains well separated Mn^{2+} (d^5, $S = 5/2$) spins. Therefore the Curie constant is now quantitatively explained as the sum contribution of nearly free spins on the Mn^{2+} ions and the Pauli paramagnetism from the conduction electrons. Otherwise the Curie constant is too small to explain as the sum contribution from the localized π-radical ($1.5 \times ET^{0.66+}$) and Mn^{2+} ($S = 5/2$) species. The conduction electrons actually show metallic behaviour in the reflectance spectra (discussed below).

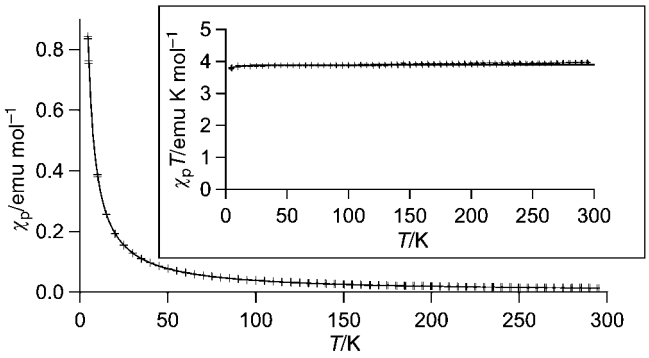

Fig. 5 The temperature dependence of the magnetic susceptibility of $(ET)_3(MnCl_4)(TCE)$. The crosses are observed data and lines are the best fitting curve using the Curie–Weiss model (see text).

The apparent inconsistency between the magnetic and electrical behaviour can be explained based on the fact that the interaction between conduction and localized electrons is very small and thus the two kinds of electrons behave rather independently. Accordingly the conduction electrons' behaviour is mainly observed in the electrical resistivity measurement, while that of the localized electrons are observed in the magnetic measurement. Because the localized electrons on each $[MnCl_4]^{2-}$ anion are already isolated enough from each other and thus behave paramagnetically, a structural transition could not alter their magnetic behaviour as a whole, while it could have an observable effect on the electrical behaviour.

The EPR spectra on the single crystal were measured to analyze the magnetic behaviour of the π- and d-electrons' contributions. Information on the behaviour of the conduction electrons was analysed best on the spectra where the external magnetic field was applied parallel to the conduction sheet (*ac*-plane) of the crystal rather than otherwise, by consideration of the Lorentz force due to the external magnetic field against the movement of the conduction electrons. The temperature dependence of peak-to-peak linewidths (ΔH_{pp}/gauss) and spin susceptibilities as well as g-values of parallel (//) and

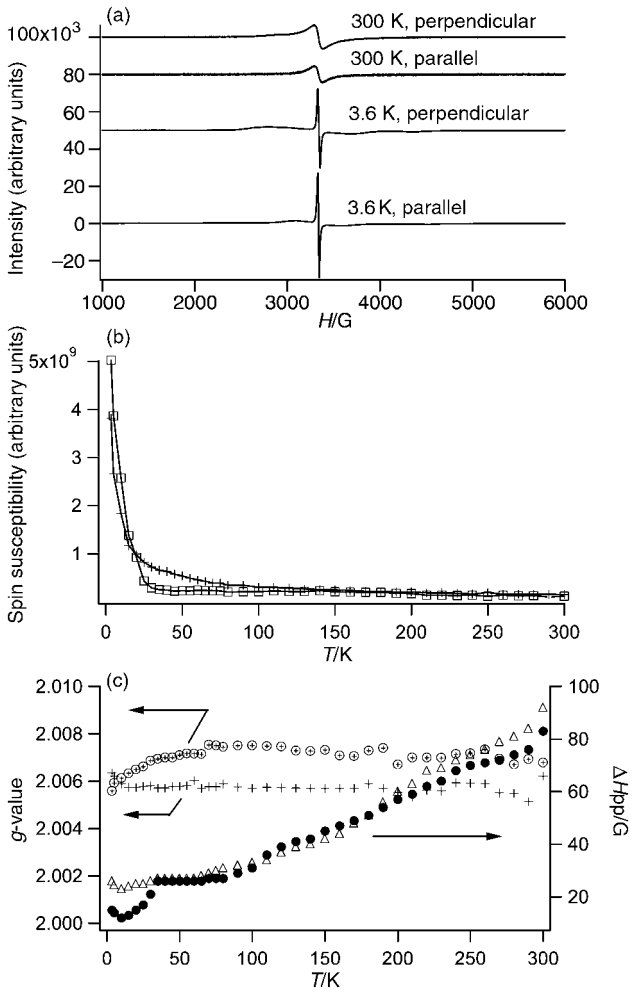

Fig. 6 The EPR spectra of the single crystal of $(ET)_3(MnCl_4)(TCE)$: (a) the line shape at 300 K and 3.6 K: note that the intensity of the two spectra at 300 K are arbitrarily multiplied for clarity, (b) temperature dependence of the spin susceptibility (parallel: square, perpendicular: cross), and (c) temperature dependence of the linewidth ΔH_{pp} (parallel: filled-circle, perpendicular: open triangle) and the g-value (parallel: cross, perpendicular: circled cross). In each figure parallel and perpendicular mean that the magnetic field was applied parallel and perpendicular to the conduction sheet (*ac*-plane), respectively.

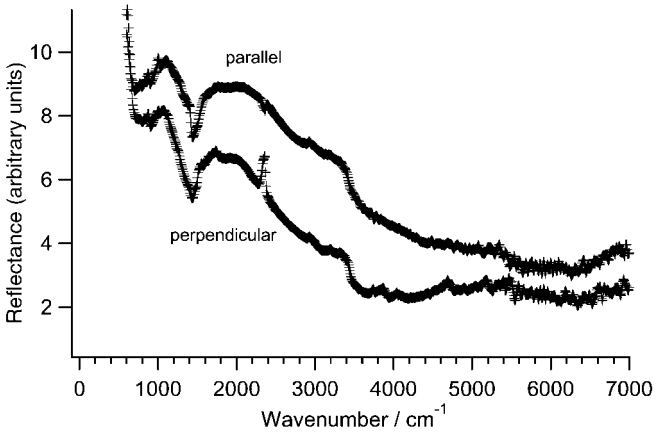

Fig. 7 The polarized reflectance spectra of $(ET)_3(MnCl_4)(TCE)$ at room temperature: the polarization is nearly parallel and perpendicular to the [10$\bar{1}$] direction.

perpendicular ($\perp$) field directions to the conduction sheet (*ac*-plane) are shown in Fig. 6. The spectra showed a single Lorentzian signal except at very low temperature ($\leqslant$15 K), where the signal can be well described as two overlaid peaks, one broad and one narrow (Fig. 6). The broad peak can only just be distinguished at low temperature. Above 30–40 K the observed spin susceptibility was almost temperature-independent, while it rapidly increased at lower temperature. Such behaviour is more obvious in the //-spectra than in the $\perp$-spectra. Thus it can be considered that the EPR signal at high temperature should come mainly from the conduction π-electrons rather than the local spins on the Mn^{2+} species, and *vice versa* at low temperature. This behaviour can be explained as follows: Curie-like behaviour of the local spins overwhelmed the Pauli-paramagnetism of the conduction π-electrons at low temperature. This explanation is consistent with the above-mentioned interpretation of static magnetic susceptibility.

As for the *g*-value, $g(\perp)$ is larger than $g(//)$ over almost the whole temperature range measured. The *g*-value $g(\perp)$ remained nearly constant down to 65 K, where the anomaly in the electrical behaviour was observed, and then it suddenly showed a downward trend. The temperature dependence of the linewidth of the spectra in either direction of the magnetic field, $\Delta H_{pp}(//)$ and $\Delta H_{pp}(\perp)$, exhibited an anomaly in the range of 35–65 K. From room temperature to 3.5 K they both decreased monotonously with decreasing temperature except between 35 and 65 K; they suddenly become constant in this range of temperature. This temperature range of the anomaly coincides with those of the other observations mentioned above.

Optical properties

The preliminary reflectance spectra measured at room temperature are shown in Fig. 7. Though the spectra are noisy at wavenumbers higher than *ca.* 5500 cm^{-1} due to the rough surface of the specimen, they clearly manifest Drude-like dispersions in both directions of the polarization at wavenumbers lower than *ca.* 4000 cm^{-1}, and this proves that the material has metallic conduction electrons around room temperature. The spectra also show us that this material has a highly isotropic electronic structure within the conduction sheet, because there is only a small difference in the reflectance spectra between the 0° and 90° polarizations. As for the temperature dependence of the reflectance spectra, we did not observe any qualitative difference in the spectra above 65 K. Therefore we can conclude from the optical results that this material keeps metallic electronic structure at least above the structural transition temperature.

Concluding remarks

A new molecular conductor β''-$(ET)_3(MnCl_4)(1,1,2\text{-}C_2H_3Cl_3)$ is located at the marginal region between metals and semiconductors, and exhibits unusual and complicated physical properties. The interaction between conduction electrons and local spins is very small and they behave almost independently. On the other hand the interaction between both electronic systems and the lattice is not negligible. Therefore the electrical and magnetic properties might be controllable by pressure. At the same time a perturbation which can selectively modulate the energy of a particular system (conduction electrons, local spins or lattice), *e.g.* magnetic field applied parallel/perpendicular to the conduction sheet, could also affect the physical properties in a unique way. In these respects a study of the electrical and magnetic properties under high pressure and magnetic field would be intriguing and is actually now under way. This new molecular conductor could be a prospective candidate for multi-controllable functional materials.

Acknowledgements

One of the authors (T. N.) thanks Dr M. Wakeshima and Professor Y. Hinatsu at Hokkaido University for their help in the magnetic susceptibility measurements and also thanks Professors T. Mori (Tokyo Institute of Technology) and H. Mori (International Superconductivity Technology Center) for their helpful discussion on the crystal structure. This work was partly supported by a Grant-in-Aid for Scientific Research from the Ministry of Education, Culture, Sports, Science and Technology.

References

1 For example, see *ICSM'98 on CD-ROM*, Elsevier Science, 1998, and references cited therein.
2 P. Day, M. Kurmoo, T. Mallah, I. R. Marsden, R. H. Friend, F. L. Pratt, W. Hayes, D. Chasseau, J. Gaultier, G. Bravic and L. Ducasse, *J. Am. Chem. Soc.*, 1992, **114**, 10722.
3 M. Kurmoo, A. W. Graham, P. Day, S. J. Coles, M. B. Hursthouse, J. L. Caulfield, J. Singleton, F. L. Pratt, W. Hayes, L. Ducasse and P. Guionneau, *J. Am. Chem. Soc.*, 1995, **117**, 12209.
4 L. Martin, S. S. Turner, P. Day, K. M. A. Malik, S. J. Coles and M. B. Hursthouse, *Chem. Commun.*, 1999, 513.
5 E. Coronado, J. R. G.-Mascaros, C. J. Goméz-García and V. Laukhin, *Nature*, 2000, **408**, 447.
6 H. Kobayashi, A. Kobayashi and P. Cassoux, *Chem. Soc. Rev.*, 2000, **29**, 325.
7 M. Matsuda, T. Naito, T. Inabe, N. Hanasaki, H. Tajima, T. Otsuka, K. Awaga, B. Narymbetov and H. Kobayashi, *J. Mater. Chem.*, 2000, **10**, 631.
8 S. Uji, H. Shinagawa, C. Terakura, T. Terashima, T. Yakabe, Y. Terai, M. Tokumoto, A. Kobayashi, H. Tanaka and H. Kobayashi, *Nature*, 2001, **410**, 908.
9 T. Lis, *Acta Crystallogr. Sect. B*, 1980, **36**, 2042.
10 R. Sessoli, H.-L. Tsai, A. R. Schake, S. Wang, J. B. Vincent, K. Folting, D. Gatteschi, G. Christou and D. N. Hendrickson, *J. Am. Chem. Soc.*, 1993, **115**, 1804.
11 H. J. Eppley, H.-L. Tsai, N. de Vries, K. Folting, G. Christou and D. N. Hendrickson, *J. Am. Chem. Soc.*, 1995, **117**, 301.
12 P. D. W. Boyd, Q. Li, J. B. Vincent, K. Folting, H.-R. Chang, W. E. Streib, J. C. Huffman, G. Christou and D. N. Hendrickson, *J. Am. Chem. Soc.*, 1988, **110**, 8537.
13 K. Takeda, K. Awaga and T. Inabe, *Phys. Rev. B*, 1998, **57**, R11062.
14 K. Takeda, PhD Thesis, The University of Tokyo, 1999.
15 *SIR92*, A. Altomare, M. C. Burla, M. Camalli, M. Cascarano, C. Giacovazzo, A. Guagliardi and G. Polidori, *J. Appl. Crystallogr.*, 1994, **27**, 435.
16 D. T. Cromer and J. T. Waber, *International Tables for X-ray Crystallography*, vol. IV, The Kynoch Press, Birmingham, England, Table 2.2 A, 1974.

17 D. C. Creagh and J. H. Hubbell, *International Tables for Crystallography*, vol. C, ed. A. J. C. Wilson, Kluwer Academic Publishers, Boston, Table 4.2.4.3, 1992, pp. 200–206.
18 *teXsan*, Crystal Structure Analysis Package, Molecular Structure Corporation, 1985 & 1992.
19 L. J. Farrugia, *J. Appl. Crystallogr.*, 1997, **30**, 565; the program is available from the following URL, http://www.chem.gla.ac.uk/~louis/ortep3/.
20 T. Mori, *Bull. Chem. Soc. Jpn.*, 1998, **71**, 2509.
21 M. J. Rosseinsky, M. Kurmoo, D. R. Talham, P. Day, D. Chasseau and D. Watkin, *J. Chem. Soc., Chem. Commun.*, 1988, 88.
22 U. Geiser, J. A. Schlueter, H. H. Wang, A. M. Kini, J. M. Williams, P. P. Sche, H. I. Zakowicz, M. L. Vanzile, J. D. Dudek, P. G. Nixon, R. W. Winter, G. L. Gard, J. Ren and M.-H. Whangbo, *J. Am. Chem. Soc.*, 1996, **118**, 9996.
23 T. Mori and H. Inokuchi, *Bull. Chem. Soc. Jpn.*, 1988, **61**, 591.
24 T. Mori, P. Wang, K. Imaeda, T. Enoki, H. Inokuchi, F. Sakai and G. Saito, *Synth. Met.*, 1988, **27**, A451.
25 K. A. Abboud, M. B. Clevenger, G. F. de Oliveira and D. R. Talham, *Chem. Commun.*, 1993, 1560.
26 P. Guinneau, C. J. Kepert, D. Chasseau, M. R. Truter and P. Day, *Synth. Met.*, 1997, **86**, 1973.